Thermodynamic Performance of Regenerative Organic Rankine Cycles

Kyoung Hoon Kim[1]

Abstract—ORC (Organic Rankine Cycle) has potential of reducing consumption of fossil fuels and has many favorable characteristics to exploit low-temperature heat sources. In this work thermodynamic performance of ORC with regeneration is comparatively assessed for various working fluids. Special attention is paid to the effects of system parameters such as the turbine inlet pressure on the characteristics of the system such as net work production, heat input, volumetric flow rate per 1 MW of net work and quality of the working fluid at turbine exit as well as thermal efficiency. Results show that for a given source the thermal efficiency generally increases with increasing of the turbine inlet pressure however has optimal condition for working fluids of low critical pressure such as iso-pentane or n-pentane.

Keywords—low-grade energy source, organic Rankine cycle (ORC), regeneration, Patel-Teja equation.

I. INTRODUCTION

SINCE it is impossible to converse low grade energy to electricity efficiently by conventional methods, most of the low grade energy are just discarded. Therefore the research is important how to generate electricity efficiently from low grade energy sources. In recent years, organic Rankine cycle has become a field of intense research and appears as a promising technology for conversion of heat into useful work of electricity. In an ORC the saturation vapor curve is the most crucial characteristics of a working fluid. This characteristic affects the fluid applicability, cycle efficiency, and arrangement of associated equipment in a power generation system [1-2].

Schuster et al [3] mention numerous running applications, such as geothermal power plant, biomass fired combined heat and power plants, solar desalination plants, waste heat recovery or micro CHP. Drescher and Bruggemann [4] investigate the ORC in solid biomass power and heat plants. They propose a method to find suitable thermodynamic fluids for ORCs in biomass plants and found that the family of alkylbenzenes showed the highest efficiency. Dai et al [5] use a generic optimization algorithm, identified isobutane and R236ea as efficient working fluids. Heberle and Brueggemann [6] investigate the combined heat and power generation for geothermal re-sources with series and parallel circuits of an ORC.
Tranche et al. [7] investigate comparatively the performance of solar organic Rankine cycle using various working fluids. Volume flow rate, mass flow rate, power ratio as well as thermal efficiency are used for comparison. Hung et al. [8] examine Rankine cycles using organic fluids which are categorized into three groups of wet, dry and isentropic fluids. They point out that dry fluids have disadvantages of reduction of net work due to superheated vapor at turbine exit, and wet fluids of the moisture content at turbine inlet, so isentropic fluids are to be preferred. Kim [9] investigated comparatively the thermodynamic performance of ORC with superheater for various working fluids including wet, dry and isentropic fluids.

In this paper, the thermodynamic performance of ORC with regeneration is comparatively investigated for various working fluids. The various thermodynamic characteristics of the ORC such as enthalpy ratio, net work production, heat input and volume flow rate as well as thermal efficiency are investigated in terms of the parameters such as turbine inlet pressure.

II. SYSTEM ANALYSIS

The system considered in this work consists of condenser, pump, turbine, regenerator, pre-heater, boiler, and super-heater and its schematic diagram is shown in Fig. 1. The working fluids considered in this work are nine fluids of NH_3 (ammonia), R134a, R22, iC_4H_{10} (iso-butane), R152, R143a, C_4H_{10} (butane), iC_5H_{12} (iso-pentane), nC_5H_{12} (normal pentane). In this work the thermodynamic properties of the working fluids are calculated by Patel-Teja equation of state [10-11]. The basic data of the fluids which are needed to calculate Patel-Teja equation are shown in TABLE 1, where M, T_c, P_c and ω are molecular weight, critical temperature, critical pressure, and accentric factor, respectively [12]. The molecular weights of NH_3 and
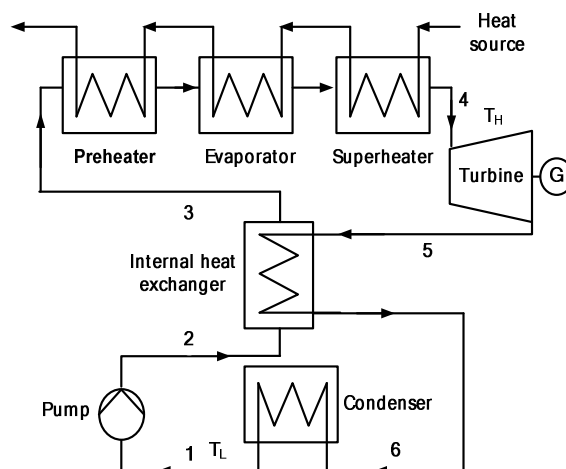

Fig. 1 Schematic diagram of the system

[1] K. H. Kim is with Dept. Mech. Eng., Kumoh National Institute of Technology, 61 Daehakro, Gumi, Gyeongbuk 730-701, Korea (phone: 82-54-478-7292; fax: 82-54-478-7319; e-mail: khkim@ kumoh.ac.kr).

World Academy of Science, Engineering and Technology
International Journal of Mechanical and Mechatronics Engineering
Vol:5, No:11, 2011

TABLE I
BASIC DATA FOR THE WORKING FLUIDS

substance	M (kg/kmol)	Tc (K)	Pc (bar)	ω
NH_3	17.031	405.65	112.78	0.252
R134a	102.031	380.00	36.90	0.239
R22	86.468	369.30	49.71	0.219
iC_4H_{10}	58.123	408.14	36.48	0.177
R152a	66.051	386.60	44.99	0.263
R143a	84.041	346.25	37.58	0.253
C_4H_{10}	58.123	425.18	37.97	0.199
iC_5H_{12}	72.150	462.43	33.81	0.228
nC_5H_{12}	72.150	469.65	33.69	0.249

iC_4H_{10} are small, and those of R123 and C_8H_{12} are large among the fluids. The critical temperatures of R143a and R22 are low and those of nC_5H_{12} and iC_5H_{12} are high. The critical pressures of nC_5H_{12} and iC_5H_{12} are low and those of NH_3 and R22 are high. The temperature-entropy diagrams for the fluids are shown in Fig. 2. It can be seen from the figure that iC_4H_{10}, C_4H_{10}, iC_5H_{12} and nC_5H_{12} belong to dry fluids, R134a and R143a to isentropic fluids, and NH_3, R22 and R152a to wet fluids. Especially, latent heat of vaporization of NH_3 is much greater than the others so the whole temperature-entropy diagram for NH_3 is not shown in the figure. The temperature-volume diagrams of the fluids are shown in Fig.3. The volume of saturated vapor at a given temperature is large for nC_5H_{12} or iC_5H_{12}, and small for R143a or R22.

A low-grade sensible energy is supplied to the system and important assumptions used in this work are as follows.
1) The energy source is air at temperature of T_S.
2) The working fluid leaves the condenser as saturated liquid at temperature of T_L.
3) The evaporating temperature, T_E is lower than the critical temperature of the fluid and the turbine inlet temperate becomes $T_S - \Delta T_H$ by the superheater.
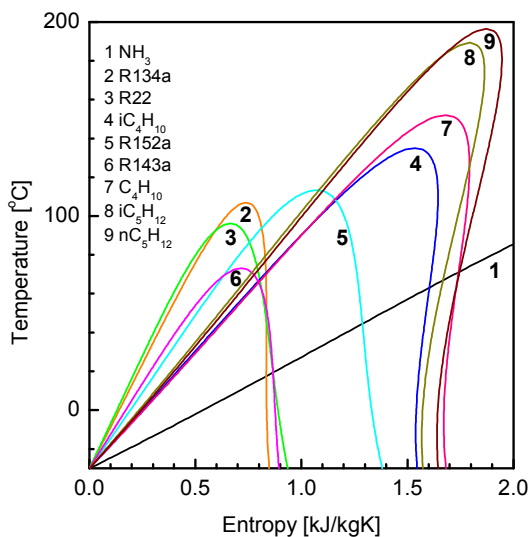4) The minimum temperature difference between the hot and cold streams in the regenerator is operated at a prescribed

pinch point, ΔT_{PP}.
5) Pressure drop and heat loss of the systems are negligible.

At point 1, the fluid is saturated liquid at T_L and the corresponding saturated pressure P_L is the low pressure of the system. When the evaporating temperature is T_E, the corresponding saturation pressure P_H is the high pressure of the system. The thermodynamic properties at point 4 are determined with the temperature T_H and the pressure P_H. The thermodynamic properties at points 2 and 5 are determined with the isentropic efficiencies of pump and turbine, η_p and η_t, respectively.

As the heat exchange area of regenerator increases, the temperature difference between the hot and cold streams, $T_{hot} - T_{cold}$, decreases and finally reaches the prescribed limit of the pinch point, ΔT_{PP}. Then the thermodynamic properties at 2 and 5 can be determined from following conditions.

$$P_2 = P_H \quad (1)$$
$$P_5 = P_L \quad (2)$$
$$h_5 - h_6 = h_3 - h_2 \quad (3)$$
$$\min(T_{hot} - T_{cold}) = \Delta T_{PP} \quad (4)$$

Then heat addition and net work per unit mass of a working fluid q_{in} and w_{net}, and thermal efficiency η_{th} are be obtained as

$$q_{in} = h_4 - h_3 \quad (5)$$
$$w_{net} = w_t - w_p = (h_4 - h_5) - (h_2 - h_1) \quad (6)$$
$$\eta_{th} = w_{net} / q_{in} \quad (7)$$

where h denotes specific enthalpy and subscripts t and p denote turbine and pump, respectively.
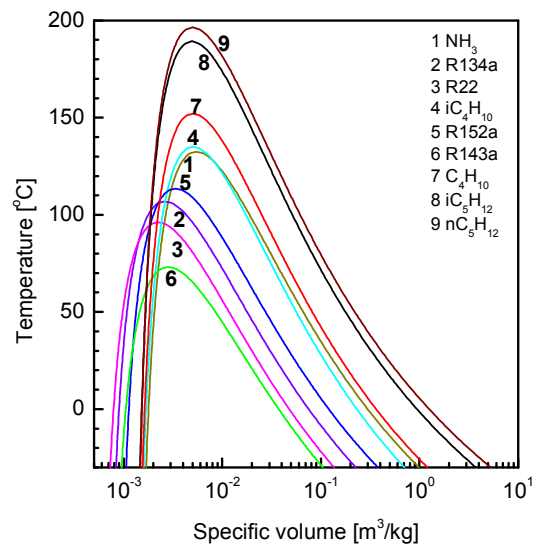
In this work enthalpy ratio, x, is defined as

Fig. 2 Temperature-entropy diagrams for the working fluids

Fig. 3 Temperature-specific volume diagrams for the working fluids

World Academy of Science, Engineering and Technology
International Journal of Mechanical and Mechatronics Engineering
Vol:5, No:11, 2011

TABLE II
BASIC CALCULATION CONDITIONS

symbol	Parameter	data	unit
T_S	source temperature	200	^oC
T_L	condensing temperature	20	^oC
ΔT_H	temperature difference at source inlet	15	^oC
ΔT_{PP}	pinch point	10	^oC
η_p	isentropic efficiency of pump	0.80	
η_t	isentropic efficiency of turbine	0.80	
	source	air	

$$x = \frac{h - h_f}{h_g - h_f} \qquad (6)$$

where h_f and h_g denote the specific enthalpy of saturated liquid and vapor of the working fluid, respectively. So when $0 \leq x \leq 1$, x is same as the quality of the fluid and the fluid is the mixture of saturated liquid and vapor. When $x < 0$, the fluid is a com-pressed liquid, and when $x > 1$, the fluid is a superheated vapor.

III. RESULTS AND DISCUSSIONS

The system parameters used in this work are summarized in Table II. In this work the basic data for analysis are $T_S = 200^oC$ and $\Delta T_H = 15^oC$, so the turbine inlet temperature in this work is fixed at $T_H = T_S - \Delta T_H = 185^oC$. Fig. 4 shows the effects of the turbine inlet pressure on the enthalpy ratio for various working fluids. It can be seen from the figure that the enthalpy ratio decreases as the turbine inlet pressure increases. Enthalpy ratio of R143a or R22 is relatively high, and that of NH_3 or nC_5H_{12} is relatively low. On the other hand, since this work is limited to the subcritical range, the turbine inlet pressure is lower than the critical pressure of the fluid so that the phase transition from liquid of vapor exists.

Fig. 5 shows the effects of the turbine inlet pressure on the temperature difference of the regenerator which is the
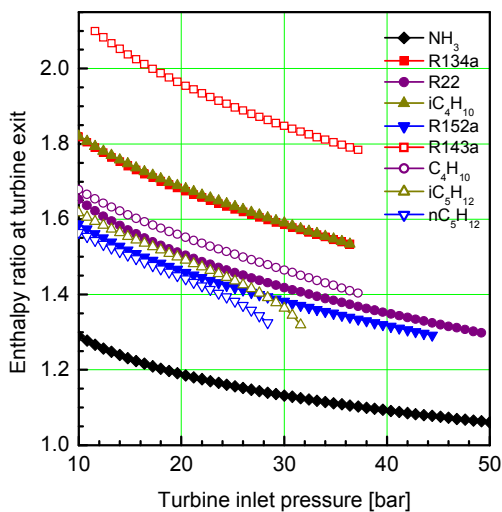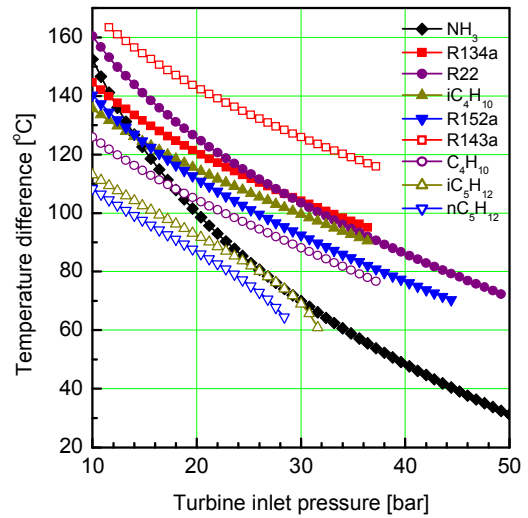

Fig. 5 Temperature difference of regenerator as a function of turbine inlet pressure

difference between the temperature at the exit of turbine and the temperature at the exit of pump. The figure shows that the temperature difference decreases as the turbine inlet pressure increases when the turbine inlet temperature is held at a constant value, since as the turbine inlet pressure increases, the enthalpy ratio at turbine inlet or exit decreases and consequently the temperature at the turbine exit decreases. For a fixed value of turbine inlet pressure, the temperature of R143a R22 is relatively high, whereas that of nC_5H_{12} or iC_5H_{12} is relatively low.

Fig. 6 shows the effects of the turbine inlet pressure on the heat input per unit mass of working fluid for various working fluids. The figure shows that for a fixed value of turbine inlet pressure the heat input generally increases with increasing of the turbine inlet pressure. However, it has an optimal value with respect to the turbine pressure for working fluids of low critical
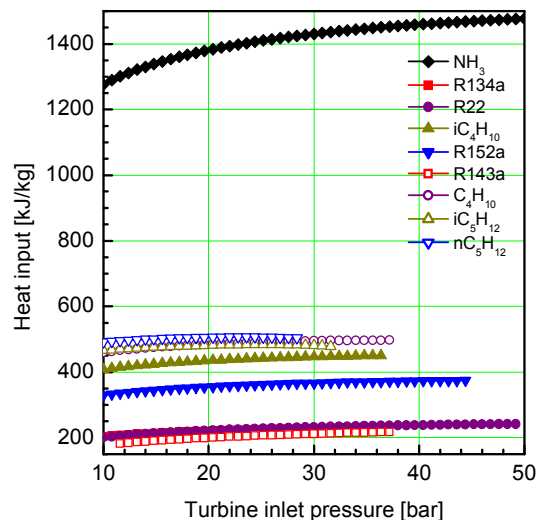

Fig. 4 Enthalpy ratio at turbine exit as a function of the turbine inlet pressure for various working fluids

Fig. 6 Heat input per unit mass of source as a function of the turbine inlet pressure for various working fluids

World Academy of Science, Engineering and Technology
International Journal of Mechanical and Mechatronics Engineering
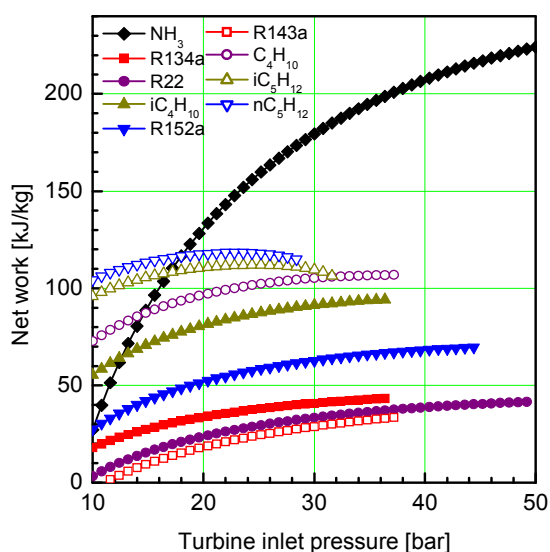Vol:5, No:11, 2011

Fig. 7 Net work per unit mass of working fluid as a function of
turbine inlet pressure for various working fluids

pressure such as iC_5H_{12} or nC_5H_{12}. Heat input of NH_3, is much higher than that of other working fluids, whereas heat input of R143a or R22 is relatively low.

Fig. 7 shows the effects of the turbine inlet pressure on the net work per unit mass of fluid for various working fluids. The figure shows that the net work per unit mass of fluid generally increases as the turbine inlet pressure increases. Net work of NH_3 is much higher than those of other fluids in the range of high turbine inlet pressure, and net work of nC_5H_{12} or iC_5H_{12} is relatively high, and R22 or R143a is relatively low. In the case of nC_5H_{12} or iC_5H_{12}, there exists an optimal value of the net work with respect to the turbine inlet pressure.

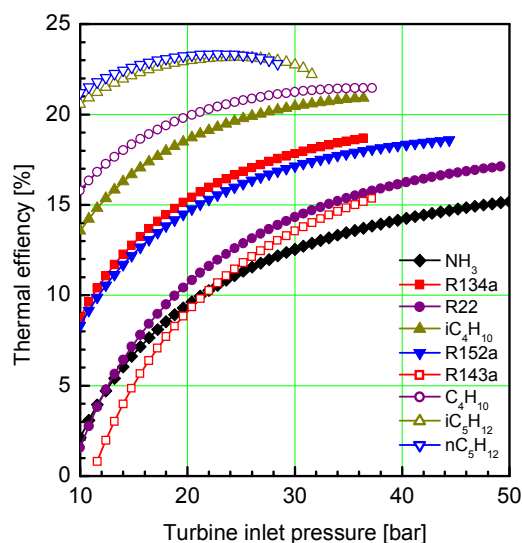Fig. 8 shows the effects of the turbine inlet pressure on the

Fig. 8 Thermal efficiency as a function of the turbine inlet
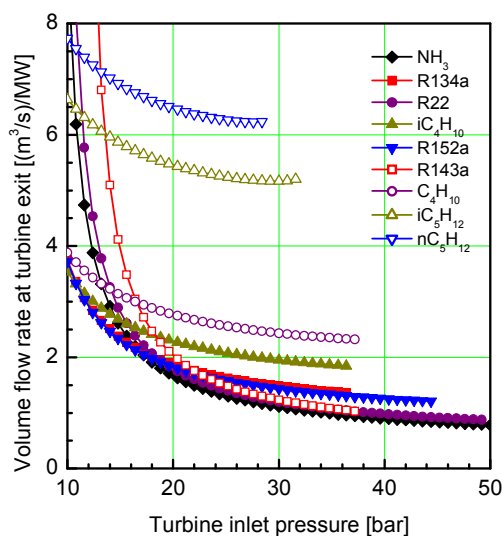pressure for various working fluids

Fig. 9 Volume flow rate of working fluid at turbine exit to produce
1MW of electricity as a function of the turbine inlet pressure

thermal efficiency for various working fluids. The figure shows that the thermal efficiency generally increases with the turbine inlet. For a fixed value of turbine inlet pressure, thermal efficiency of nC_4H_{10} or iC_5H_{12} is relatively high, whereas that of R143a or NH_3 is relatively low.

Fig. 9 shows the effects of the turbine inlet pressure on the volume flow rate at the turbine exit to produce 1 MW of net work for various working fluids. It can be seen from the figure that the volume flow rate of a working fluid to produce the same amount of net work decreases as the turbine inlet pressure increases, and the decreasing rate of the flow rate are relatively high for NH_3, R22 and R143a. Since the volume flow rate to produce a same amount of net work relates directly with the size or cost of the turbine, the volume flow rate may be an important fact for selection of a working fluid for a system.

IV. CONCLUSION

In this paper, the performance of organic Rankine cycle with regeneration has been thermodynamically analyzed. The main results are as follows:

1) As turbine inlet pressure increases for a fixed source temperature, net work per unit mass of working fluid or thermal efficiency generally increases, however, has an optimal value for working fluids which have low critical pressures.

2) The volume flow rate per 1 MW of net work would be a criterion for selection of working fluid, and its decreasing rate are relatively high for NH_3, R22 and R143a.

3) There is no working fluid which is the best for every aspect of thermodynamic performance. Therefore, in order to select an optimal working fluid for a system, various thermodynamic properties should be synthetically and comparatively considered.

REFERENCES

[1] N. A. Lai, M. Wendland, and J. Fisher, "Working fluids for high temperature organic Rankine cycle," *Energy*, vol. 36, pp. 199-211, 2011.

[2] T. C. Hung, T. Y. Shai, and S. K. Wang, "A review of organic Rankine cycles (ORCs) for the recovery of low-grade waste heat," *Energy*, vol. 22, pp. 661-667, 1997.

[3] A. Schuster, S. Karellas, and H. Splithoff, "Energytic and economic investigation of innovative Organic Rankine Cycle applications," *App. Therm. Eng.*, vol. 29, pp. 1809-1817, 2008.

[4] U. Drescher and D. Brueggemann, "Fluid selection for the organic Rankine cycle (ORC) in biomass power and heat plants," *App. Therm. Eng.*, vol. 27, pp. 223-228, 2007.

[5] Y. Dai, J. Wang, and L. Gao, "Parametric optimization and comparative study of organic Rankine cycle (ORC) for low grade waste heat recovery," *Energy Convs. Mgmt.*, vol. 50, pp. 576-582, 2009.

[6] F. Heberle and D. Brueggemann, "Exergy based fluid selection for a geothermal organic Rankine cycle for combined heat and power generation, *App. Therm. Eng.*, vol. 30, pp. 1326-1332, 2010.

[7] B. F. Tchanche, G. Papadakis, and A. Frangoudakis, "Fluid selection for a low-temperature solar organic Rankine cycle," *App. Therm. Eng.* vol. 29, pp. 2468-2476, 2009.

[8] T. C. Hung, S. K. Wang, C. H. Kuo, B. S. Pei, and K. F. Tsai, "A study of organic working fluids on system efficiency of an ORC using low-grade energy sources," *Energy*, vol. 35, pp. 1403-1411, 2010.

[9] K. H. Kim, "Effects of superheating on thermodynamic performance of organic Rankine cycles," *WASET*, vol. 78, pp. 608-612, 2011.

[10] T. Yang, G. J. Chen, and T. M. Guo, "Extension of the Wong- Sandler mixing rule to the three-parameter Patel-Teja equation of state: Application up to the near-critical region," *Chem. Eng. J.* vol. 67, pp. 27-36, 1997.

[11] J. Gao, L. D. Li, Z. Y. Zhu, and S. G. Ru, "Vapor-liquid equilibria calculation for asymmetric systems using Patel-Teja equation of state with a new mixing rule," *Fluid Phase Equilibria*, vol. 224, pp. 213- 219, 2004.

[12] C. L. Yaws, *Chemical properties handbook*, McGraw- Hill, 1999.